Predicting Intensity Changes Subsequent to Concentric Eyewall Events

Rachel G. Mauk, M.S.
Atmospheric Sciences Program
The Ohio State University

Abstract

Concentric eyewall events have been documented in very intense tropical cyclones with increasing frequency in the last two decades. During a concentric eyewall event, an outer (secondary) eyewall forms around the inner (primary) eyewall. Substantial structural changes usually follow: both eyewalls may survive or dissipate, or only one eyewall may survive. Improved instrumentation on aircraft and satellites greatly increases the likelihood of detecting an event. However, forecasting intensity during and after these events remains challenging. When concentric eyewall events occur near the time of landfall, the increased uncertainty in short-term intensity engenders even greater challenges to emergency preparations.

A sixteen-year (1997-2012) database of concentric eyewall events is developed by analyzing various sources. Included sources are published documents and microwave satellite imagery. Events are identified over both the North Atlantic (41 events in 25 tropical cyclones) and eastern North Pacific (17 events in 14 tropical cyclones) Oceans. About half of North Atlantic major hurricanes (winds of 100 kt or greater) form concentric eyewalls at some point during their lifetime, and about one-quarter of eastern North Pacific major hurricanes form concentric eyewalls. Climatological characteristics (location and time of year) are analyzed. Concentric eyewalls tend to occur in the southern portion of the regions; this distribution is especially apparent for cases of systems forming concentric eyewalls multiple times.

The intensity change subsequent to the concentric eyewall event (weakening, no change, or strengthening) is identified from the Best Track data. About 25% of tropical cyclones with

concentric eyewalls are stronger than at the time of formation at 12 h, 24 h, and 36 h following formation in both regions. Approximately 50% of North Atlantic concentric eyewall cases are weaker at 12 h, 24 h, and 36 h following formation. For the eastern North Pacific cases, 76% of cases were followed by weakening at 36 h. Of the 25 North Atlantic tropical cyclones which developed concentric eyewalls, 10 made landfall within 36 h of developing concentric eyewalls.

1. Introduction

Concentric eyewall formation often precedes significant intensity changes in intense tropical cyclones (TCs). Examples of concentric eyewalls have been documented since the 1940s (Jordan and Schatzle 1961, Willoughby et al. 1982). During a concentric eyewall event, a second eyewall forms at a larger radius than the original eyewall. The second eyewall contains a wind maximum, though initially it is weaker than that of the primary eyewall. Substantial structural changes usually follow, with one or both eyewalls dissipating. If the inner eyewall dissipates and the outer eyewall survives to become the primary eyewall, intensification can follow. This phenomenon is called an eyewall replacement cycle. If both eyewall dissipate, then substantial weakening usually follows. Willoughby et al. (1982) should be considered the first comprehensive documentation of concentric eyewalls and eyewall replacement cycles. Despite advances in monitoring technology (e.g., satellites and radar) and numerical modeling, concentric eyewall structures are not currently forecast with any significant skill.

Two cases of post- eyewall replacement cycle intensity change are provided next to indicate the range of possibilities. Hurricane Andrew (1992) and Hurricane Ike (2008) are among the more famous TCs to strike the U.S. Andrew completed an eyewall replacement cycle as it tracked towards Miami FL. Though Andrew's intensity decreased from 150 kt to 125 kt during

the eyewall replacement cycle, it had reintensified to 145 kt at the time of landfall (Landsea et al. 2004). If Andrew had remained over water for another few hours, it likely would have intensified further (Willoughby and Black 1996). Total U.S. damage was $46 billion (adjusted to 2010 dollars; Blake and Gibney 2011). Ike slowly completed an eyewall replacement cycle over the Gulf of Mexico, but did not reintensify afterwards. The new large eyewall did not fully contract and the inner core continued to lack organization. Ike's intensity peaked at 95 kt over the Gulf of Mexico, contrary to forecasts of strengthening to 110 kt before landfall. Ike closed 14 Gulf Coast oil refineries and destroyed more than 10 offshore oil rigs (Brown et al. 2010). Total damage was $28 billion (2010 dollars) to the U.S. Gulf Coast (Blake and Gibney 2011).

Andrew and Ike illustrate the different intensity changes that are possible following concentric eyewall events. The National Hurricane Center considers improving forecasts of intensity change one of its primary goals (Rappaport et al. 2009). Each hurricane produced unique hazards. Andrew was small, intense, and devastated a portion of southern Florida. Ike was large, weaker, and caused moderate damage over a wide swath of southeast Texas and Louisiana. Understanding why concentric eyewall events produce such different outcomes will help forecasters to better predict intensity changes. Accurately predicting these different outcomes from a concentric eyewall event will help communities to act appropriately when a hurricane is approaching.

Several recent studies analyzed the climatological characteristics of concentric eyewall formation in various regions. Hawkins and Helveston (2004) and Hawkins et al. (2006) identified TCs with concentric eyewalls in all TC regions. This paper used the standard boundaries for the North Atlantic region (the Atlantic Ocean north of 0° latitude, Caribbean Sea, and Gulf of Mexico; hereafter Atlantic) and the eastern North Pacific region (north of 0° latitude

and east of 140°W to the Mexican and Latin American coast). In the earlier paper, 40% of Atlantic TCs and 60% of eastern North Pacific TCs that reached an intensity of at least 120 kt exhibited concentric eyewalls at some point. In the later paper, 70% of Atlantic and 50% of eastern North Pacific TCs reaching an intensity of at least 120 kt exhibited concentric eyewalls at some point. The marked change in both regions as a result of adding 3 more years of data emphasizes the interannual variability in concentric eyewall frequency.

Kossin and Sitkowski (2009) documented cases of concentric eyewall formation over the Atlantic, eastern North Pacific, and central North Pacific Oceans (defined as the region from 140°W to 180°W and north of 0° latitude) between 1997-2006. They found 45 events over the Atlantic, 13 events over the eastern North Pacific, and one over the central North Pacific. Events occurred primarily during the most active months (July, August, and September). About 70% of 1997-2006 Atlantic TCs that reached an intensity of at least 100 kt exhibited concentric eyewalls at some point. In the eastern North Pacific, only about 50% of TCs during that period exhibited concentric eyewalls. The year-to-year variability in both regions was quite strong; counts ranged from 0-5 events over the Atlantic and 0-4 over the eastern North Pacific. Kuo et al. (2009) identified concentric eyewall events from 1997-2006 in the western North Pacific. Most concentric eyewall cases occur in strong typhoons (equivalent to at least Category 4 on the Saffir-Simpson Hurricane Wind Scale). However, concentric eyewall events did not always coincide with the TC's maximum intensity.

The intensity changes occurring after concentric eyewall formation have also been examined (Sitkowski et al. 2011, Kuo et al. 2009, Yang et al. 2013). Sitkowski et al. (2011) identified 24 completed eyewall replacement cycles in Atlantic Ocean hurricanes occurring from 1977-2007. They divided the eyewall replacement cycle into three phases: intensifying,

weakening, and reintensification. The average duration of the weakening phase was 16.6 h, with a 20 kt intensity decrease. The reintensification phase lasted an average of 10.7 h, and intensity increased 8 kt. Large variances in timing and intensity change were observed during these stages. During intensification, both the outer and inner wind maxima intensify and contract to some degree. Only 14 of the 24 eyewall replacement cycles in their climatology contained this phase. During weakening, the inner wind maximum begins to decay while the outer continues intensifying. The classic concentric ring structure appears on microwave imagery during this phase. During reintensification, the outer wind maximum exceeds the inner's intensity. The inner wind maximum dissipates, at which point the authors consider the eyewall replacement cycle complete.

To analyze the formation of concentric eyewall structure, Kuo et al. (2009) focused on the 24 h before and after concentric eyewalls were identified on microwave imagery. Cases were divided into negative and positive intensity trends for each period. About half of concentric eyewall cases increased in intensity during the 24 h prior and decreased in the subsequent 24 h. Roughly equal numbers had consistent intensity changes during the two periods (increasing or decreasing). Only two of the cases decreased in intensity and then increased.

Yang et al. (2013) performed a follow-up study to Kuo et al. (2009). Methods were very similar, but Yang et al. used stricter criteria for identifying concentric eyewalls on microwave imagery. They also extended the study to 2011, for a total of 70 concentric eyewall cases. Yang et al. defined three categories for concentric eyewall events: eyewall replacement cycle, no replacement cycle, and concentric eyewall maintained. In eyewall replacement cycle cases (53%), the inner eyewall must dissipate within 20 h of concentric eyewall formation. In no replacement cycle cases (24%), the outer eyewall must begin to dissipate within 20 h of

formation. In concentric eyewall maintained cases (23%), the concentric eyewall structure must be maintained for at least 20 h.

This paper investigates recent concentric eyewall events, with a particular focus on the intensity changes occurring after each event. The following questions will be addressed:

- What are the climatological characteristics of 1997-2012 concentric eyewall events over the Atlantic and eastern North Pacific Oceans?
- What intensity changes occur in the 36 h following concentric eyewall formation?

In Section 2, the data used in this study are documented. Section 3 will discuss aspects of the methodology. Section 4 presents the results, focusing on the two questions above. Section 5 summarizes the work and discusses future areas of inquiry.

2. Data

HURDAT (Jarvinen et al. 1984) is the official record of tropical and subtropical cyclone position and intensity for systems that are within the area monitored by the National Hurricane Center. Every six hours, the latitude/longitude, maximum wind speed, sea-level pressure, and classification (low, subtropical, tropical, extratropical) are recorded. The latest version (HURDAT2) also contains the radius of 34-, 50-, and 64-kt winds in four quadrants (Landsea and Franklin 2013). New systems are added once all available information has been analyzed to produce the "best track" data. An ongoing reanalysis project (see Landsea et al. 2004 as an example) produces updates to TCs from the early part of the record. Versions are available from the National Hurricane Center's website for both the Atlantic Ocean and the eastern and central North Pacific Ocean. The Atlantic record begins in 1851, and the eastern North Pacific in 1949.

The National Hurricane Center produces a report on each TC within a few months of its occurrence. It includes the synoptic history, meteorological statistics, casualty and damage statistics, forecast and warning critique, and relevant tables and plots. For a sample, the reader is directed to the Hurricane Irene report (Avila and Cangialosi 2011). Summaries of individual TCs in a given season are published in the American Meteorological Society journal *Monthly Weather Review*. This paper often contains similar information to the TC report. The *Monthly Weather Review* summary will be cited preferentially for a given TC unless the TC Report contains additional information.

Infrared (IR) and visible satellite data is useful for tracking TCs and for evaluating intensity through the Dvorak technique (Dvorak 1975, 1984; Velden et al. 2006). However, both data types are limited in usefulness for determining structure when a cirrus canopy is present. IR collects only the temperatures of the top layer of clouds, and visible wavelengths cannot penetrate either. A developing eye and eyewall can be obscured by cirrus. Microwave imagery provides an additional data source: it can penetrate through clouds to reveal the internal structure of the TC. The eye, eyewall, and rainbands are readily discernible on microwave imagery. The various forms of atmospheric water (vapor, ice, raindrops) have differing emissivities and scattering properties, and thus appear distinct on microwave imagery (Negri et al. 1989; Lee et al. 2002).

Microwave sensors' usefulness for research and operations is severely restricted by their orbit. The sensors are usually mounted aboard polar-orbiting satellites. A narrow swath of data is available at irregular intervals. While the number of microwave sensors in operation has increased dramatically since the mid-1990s, coverage is still spotty. A TC may be captured in several passes over a few hours. In other cases, nearly a day can elapse before a satellite catches

the TC again. The Naval Research Laboratory TC archive (Hawkins et al. 2001) contains available microwave passes capturing TCs from late 1997 to the present; images are approximately centered on the TC. All images used in this project came from this archive. Since the archive begins in 1997, the start year for this project is also 1997. If the criteria discussed in Section 3 could be assessed (i.e., the image captured at least the inner core of the TC), the image was analyzed. Images from the following instruments were used: Special Sensor Microwave/Imager (SSMI, 1997-2012 seasons), TRMM Microwave Imager (TMI, 1998-2012 seasons), Special Sensor Microwave Imager/Sounder (SSMIS, 2006-2012 seasons), Advanced Microwave Scanning Radiometer for EOS (AMSR-E, 2003-2011 seasons). Passes from WindSat and the Advanced Microwave Sounding Unit-B (AMSU-B) are available as well, but are not used in this study. WindSat does not have the 85-91 GHz channel, and AMSU-B's resolution is too coarse to view concentric eyewalls.

3. Methods

Six studies have used microwave imagery to identify concentric eyewall events (Hawkins and Helveston 2004; Hawkins et al. 2006; Kossin and Sitkowski 2009; Kuo et al. 2009; Hence and Houze 2012; Yang et al. 2013). Several similarities are apparent in the methodologies. Concentric eyewalls are most frequently defined as the presence of a quasi-circular ring of relatively intense convection surrounding the primary eyewall, and mostly separated by a ring of weaker convection. The outer ring can be anywhere from 62.5-100% complete to qualify as a secondary eyewall. Objective classification of concentric eyewall events based on satellite

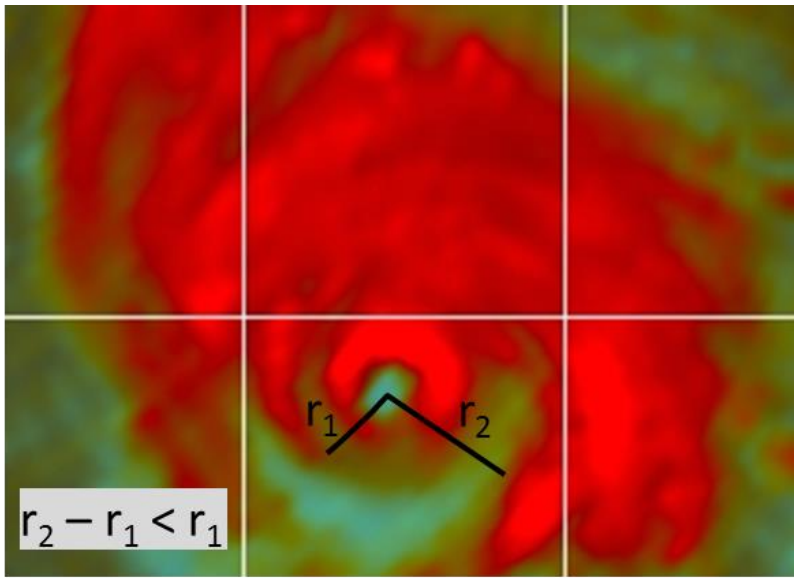

Figure 1. Diagram of the circularity criterion for identification of concentric eyewall cases. Each eyewall must meet the criterion of r_2 (radius of eyewall at two-thirds point) – r_1 (radius of near end) < r_1. This criterion eliminates spiral bands from being considered eyewalls.

imagery is far less common than subjective classification. Five of the six studies used subjective criteria. Another similarity between the studies is that they excluded TCs that were approaching land. Given the need to correctly predict intensity to ensure proper emergency preparations, it seems important to study these cases as well, albeit as a separate category.

Two criteria establishing the completeness and circularity of the eyewalls were used for this project. Both the inner and outer eyewalls had to be at least 67% complete (two-thirds of a circle). To establish circularity (e.g., eliminate cases of spiral rainbands), the difference between the radius of the near eyewall end (r_1) and the radius of the two-thirds point on the eyewall on its inner side (r_2) had to be less than r_1. Figure 1 depicts the measurements needed for the circularity criterion. These measurements were made using the image analysis software ImageJ (Schneider et al. 2012). The concentric eyewall event was defined to start when concentric eyewalls meeting the two criteria above appeared on satellite imagery. The concentric eyewall event was defined to end when no more than one-third of an eyewall (inner or outer) remained intact.

Satellite imagery rarely coincided with the available data in HURDAT2 (every six hours at 0000 UTC, 0600 UTC, 1200 UTC, and 1800 UTC). Therefore the start time of the concentric eyewall event from satellite imagery had to be adjusted to match available HURDAT2 times. In most cases, the satellite pass occurred between two HURDAT2 points. If the start time occurred no more than five hours after the prior HURDAT2 time, the analysis start time (abbreviated t+0 in this paper) was set to the prior HURDAT2 time. If a start time occurred between five and six hours after the prior time (or no more than one hour before the following time) then t+0 was matched to the following time. For example, if the start time occurred at 1625 UTC, t+0 would be set to 1200 UTC. If the start time occurred at 1705 UTC, t+0 would be set to 1800 UTC. Visual examination of cases supported the breakpoint at five hours. Concentric eyewall events tended to be very well developed on satellite imagery, suggesting that the structure had been in place for several hours.

Figure 2 depicts Hurricane Frances (2004) undergoing back-to-back concentric eyewall events (c.f. Franklin et al. 2006). Figure 2(a-f) depicts the first concentric eyewall event, during which Frances maintained its intensity. In this image sequence, concentric eyewalls are first visible in Fig. 2c. The inner eyewall has partially eroded in Fig. 2e, and has completely dissipated in Fig. 2f. Only 12.5 h elapsed between Fig. 2c and Fig. 2f. Frances is left with a slightly larger eye (compare Fig. 2b with Fig. 2f). Figure 2(h-n) depicts the second concentric eyewall event, during which Frances weakened by 20 kt. This concentric eyewall event lasted far longer (27 h) and Frances' inner core became much less organized. Both the inner and outer eyewalls had partially eroded by the time of Fig. 2n.

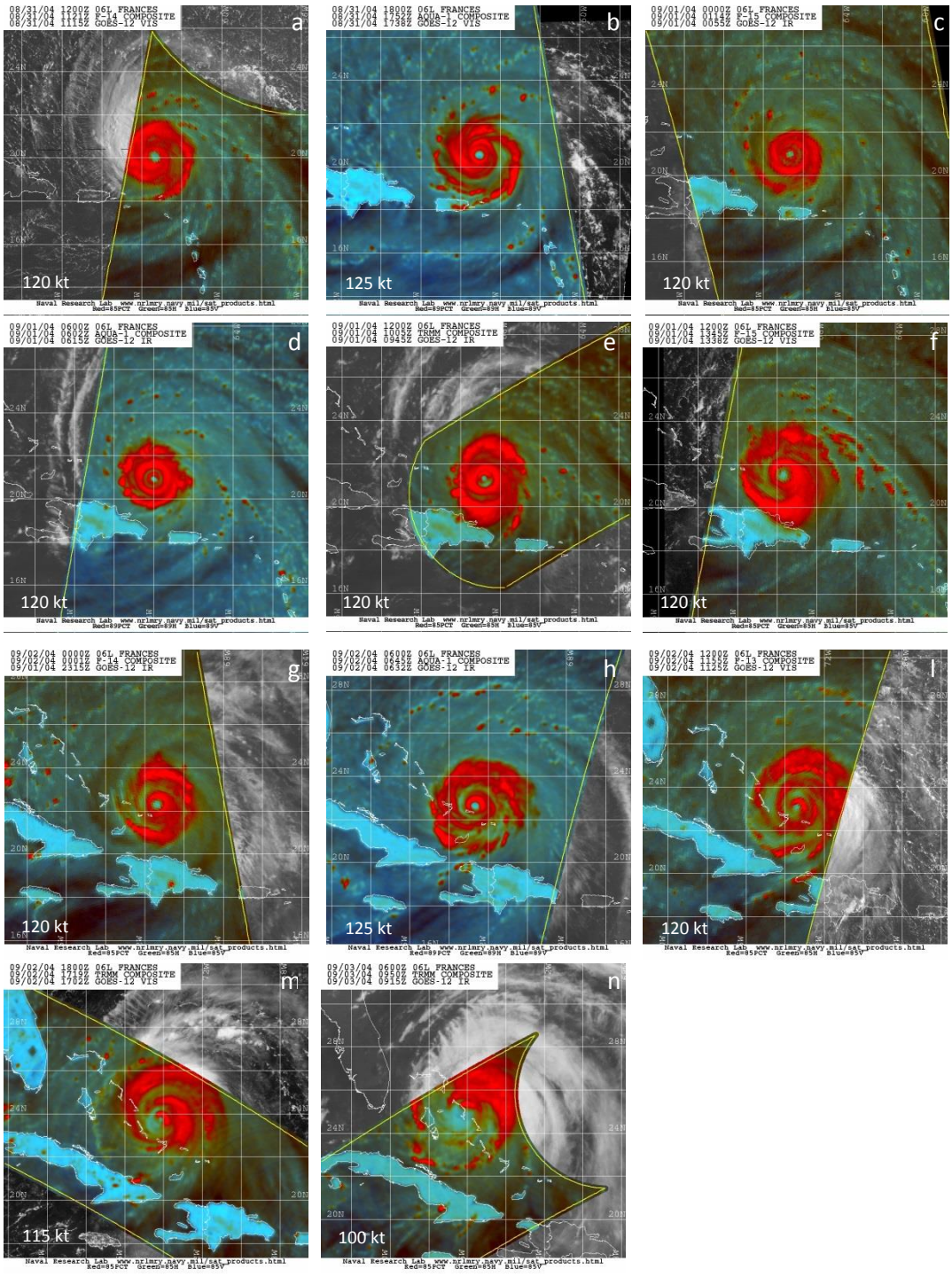

Figure 2. Sequence of satellite imagery showing two concentric eyewall cycles for Hurricane Frances, 1200 UTC 31 August 2004 – 0600 UTC 3 September 2004. Panels (a) – (f) illustrate the first concentric eyewall event, and panels (h) – (n) illustrate the second event (Table 1). Intensity at the closest synoptic time is shown in the lower left-hand corner of each image. Imagery courtesy Naval Research Labs, http://www.nrlmry.navy.mil/TC.html.

4. Results

Based on the criteria described above, 58 concentric eyewall events were identified in 39 hurricanes during the study period. Over the Atlantic Ocean, 41 concentric eyewall events were identified in 25 hurricanes. Eleven of those hurricanes produced two to five events each (27 events total). Three hurricanes produced 11 events, all within a period of 23 days during the 2004 season (Franklin et al. 2006). Over the eastern North Pacific Ocean, 17 concentric eyewall events were identified in 14 hurricanes. Three hurricanes produced two events each. Similar numbers of TCs formed in each region during the study period (267 Atlantic TCs, 289 eastern North Pacific TCs). Concentric eyewall events thus appear to be less common in the eastern North Pacific.

All concentric eyewall events occurred in hurricanes that reached maximum sustained wind speeds of 100 kt or higher (major hurricane threshold) for at least two consecutive HURDAT2 observations at some point during their lifetimes. About 45% of Atlantic major hurricanes and 28% of eastern North Pacific major hurricanes occurring from 1997-2012 exhibited concentric eyewalls at least once during their lifetimes. Most events occurred while the TC was at major hurricane status. The major hurricane period is defined as the interval beginning 6 h after the TC reaches major hurricane status. Examination of initial concentric eyewall cases over the Atlantic revealed that 72% of events occurred during the major hurricane period, 16% occurred before, and 12% occurred after. TCs that underwent multiple concentric eyewall events had a very similar distribution of cases (74%, 15%, and 11%, respectively). TCs that exhibited a single concentric eyewall event were distributed slightly differently, however (64%, 14%, and 22%, respectively). The increased proportion of single concentric eyewall events occurring after the major hurricane period may indicate that an aspect of the weakening process (perhaps the environment) is sometimes conducive to concentric eyewall formation. Multiple concentric

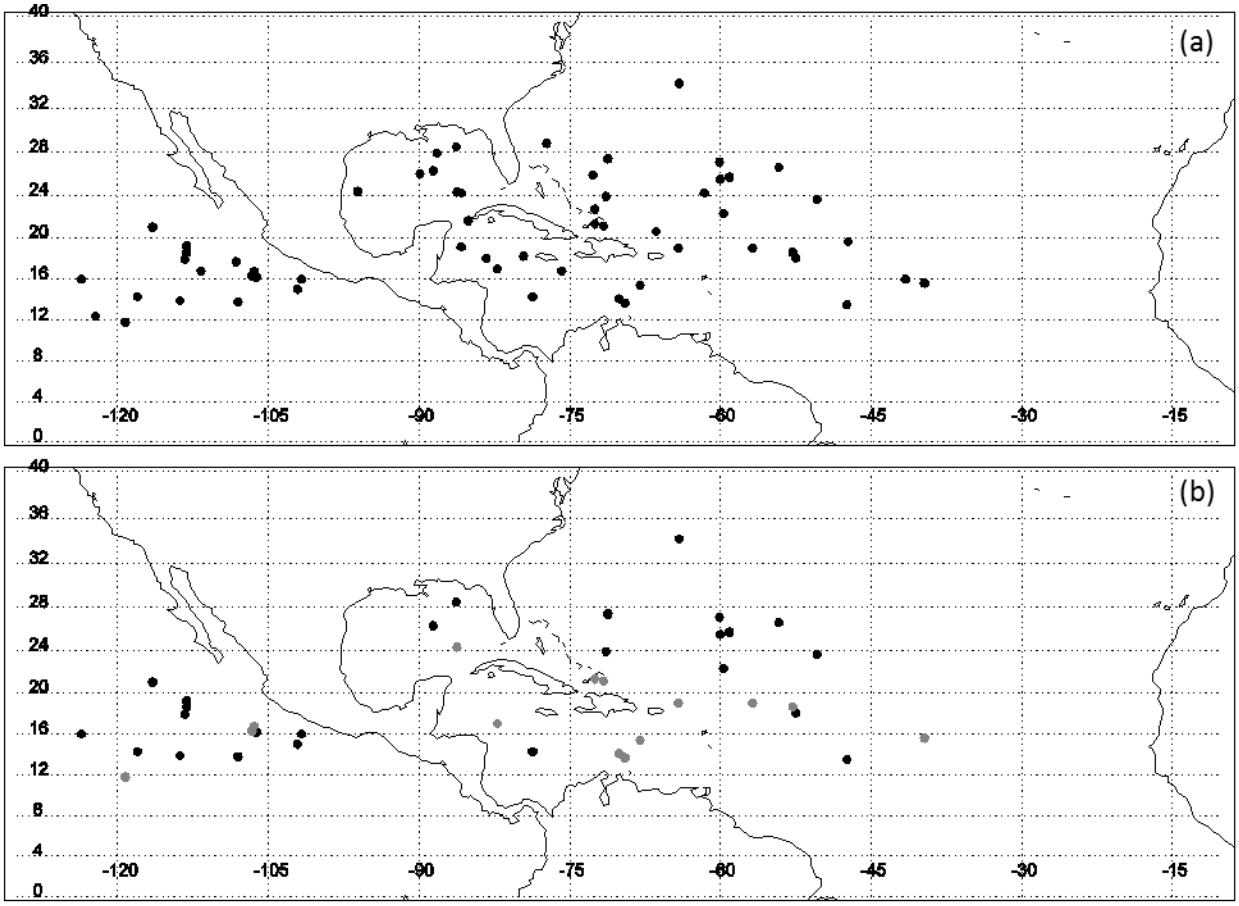

Figure 3. (a) Initial locations for the 58 concentric eyewall events (41 Atlantic, 17 eastern North Pacific). (b) Location of first concentric eyewall formation for each TC in the study (25 Atlantic, 14 eastern North Pacific). Gray dots represent TCs that underwent multiple concentric eyewall events, and the marker is placed at the location of the first concentric eyewall in the series. Black dots represent TCs that only went through one concentric eyewall event.

eyewall events are most likely when the TC maintains a very high intensity for an extended period. In the eastern North Pacific, 86% of initial concentric eyewall events occurred during the major hurricane period, 7% occurred before, and 7% occurred afterward. For the eleven single concentric eyewall cases, 91% occurred during the major hurricane period and 9% occurred afterward. For the three TCs with double concentric eyewall events, one hurricane had both

occur before the major hurricane period, and the other two had both occur during the major hurricane period.

Figure 3a shows the spatial distribution of concentric eyewall events over the Atlantic and eastern North Pacific Oceans. Over the Atlantic Ocean, concentric eyewall events occurred between 12°N - 30°N, and west of 40°W (roughly the western two-thirds of the region). Seven events (17%) occurred over the Gulf of Mexico, ten events (24%) over the Caribbean Sea, and the remaining 24 events (59%) over the Atlantic Ocean itself. Eastern North Pacific events occurred over a relatively narrow range of latitudes (12°N - 20°N); the eastern North Pacific Ocean is a small region normally, however. Figure 3b shows only the first event for each TC. If it was a single concentric eyewall event, its marker is black. If it was the first in a series of concentric eyewall events, its marker is gray. Atlantic TCs that undergo multiple concentric eyewall events tend to have their initial event at low latitudes (an average of 18°N compared to 24°N for single events). Since only three TCs undergoing multiple concentric eyewall events in the eastern North Pacific, no conclusions can be drawn about multiple events there.

Concentric eyewall events predominantly occur during late summer and early autumn over both the Atlantic and the eastern North Pacific. All Atlantic events in the study occurred from July-October, with 70% of events initiating between August 21 and September 20 (Fig. 4a). Single and multiple concentric eyewall events generally follow the same seasonal distribution (concentrated in August and September) (Fig. 4b). No single concentric eyewall event was observed after 26 September. Over the eastern North Pacific Ocean, events occurred primarily from July through September, with one event observed in late May and another in early October (Fig. 5a). Again, with only three cases of multiple concentric eyewalls in the eastern North Pacific Ocean, no conclusions can be drawn about multiple events in that region (Fig. 5b). No

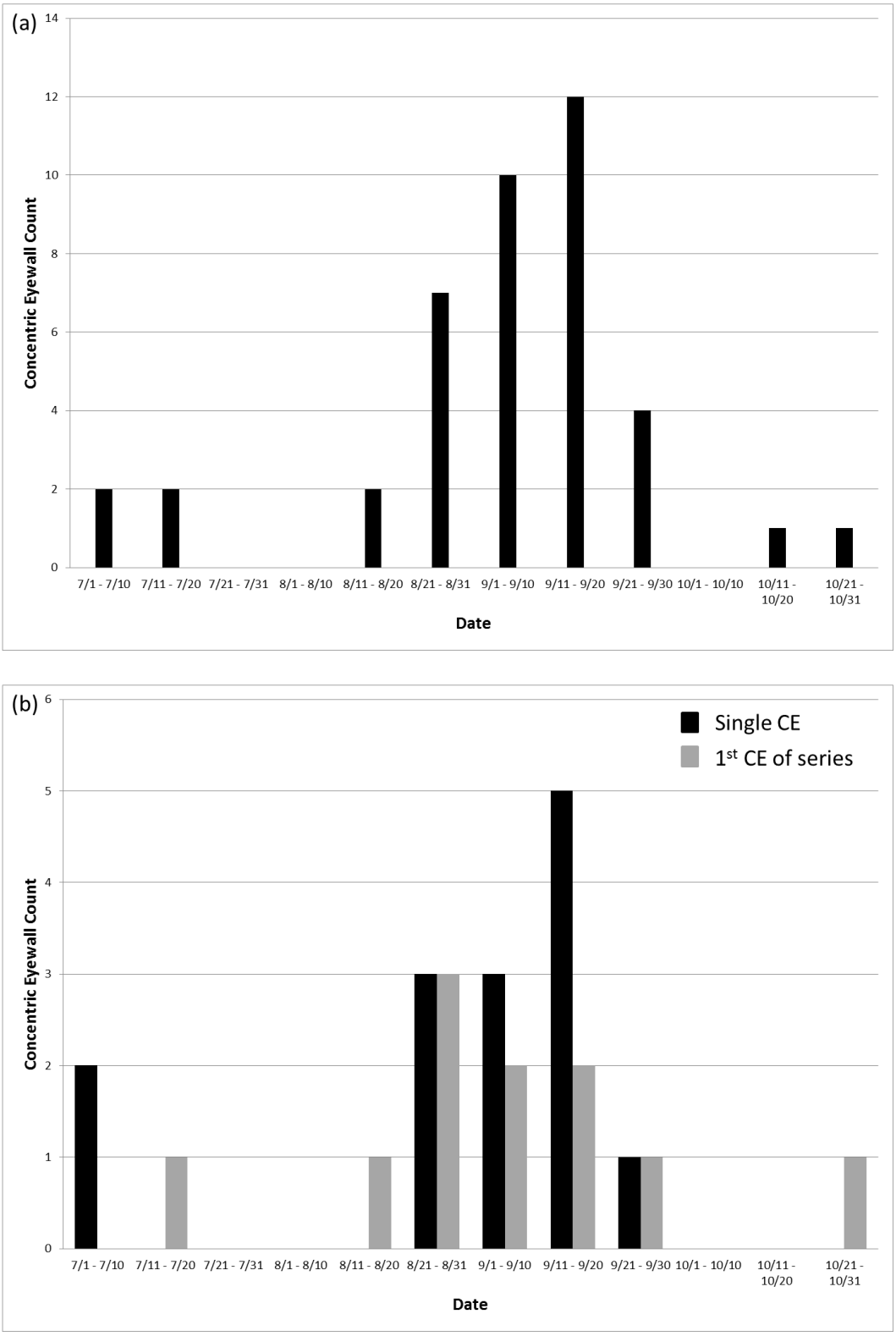

Figure 4. (a) Temporal distribution of 41 concentric eyewall events in the Atlantic Ocean. (b) Temporal distribution of 14 single concentric eyewall events (black) and 11 initial concentric eyewall events (gray).

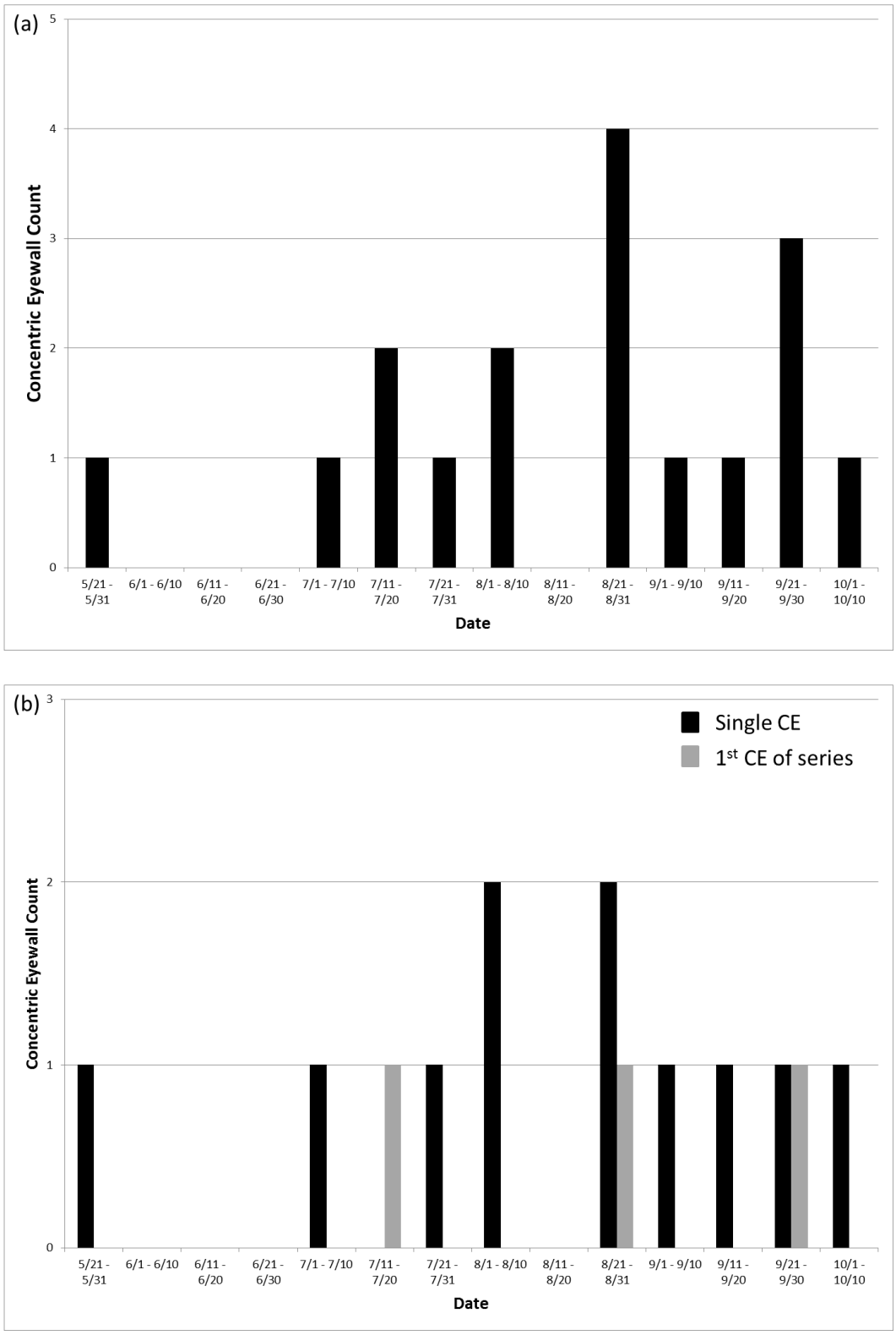

Figure 5. (a) Temporal distribution of 41 concentric eyewall events in the eastern North Pacific Ocean. (b) Temporal distribution of 14 single concentric eyewall events (black) and 11 initial concentric eyewall events (gray).

events were identified in June in either region. No major hurricanes occurred over the Atlantic Ocean in June during 1997-2012 (in fact, only three major hurricanes are recorded in HURDAT2 before 1 July), which is likely part of the reason. Five major hurricanes occurred prior to 1 July in the eastern North Pacific Ocean during 1997-2012 (sixteen total in the eastern North Pacific), so intensity does not appear to be a limiting factor. Determining the reason for no June concentric eyewall cases in the eastern North Pacific Ocean is beyond the scope of the current paper, but is an area for future work.

Operationally, the most challenging aspect of concentric eyewall events is forecasting short-term intensity. Results of an analysis of intensity changes occurring after concentric eyewall formation are presented next. Using HURDAT2 data, the maximum wind speed at the time of formation (t+0) is compared to the intensity 12 h (t+12), 24 h (t+24), and 36 h (t+36) after. Table 1 and Table 2 contain the intensity change data for the Atlantic and the eastern North Pacific, respectively. A threshold of 10 kt is used to determine significant intensity changes. An increase of 10 kt or more represents net strengthening, a decrease of 10 kt or more represents net weakening, and a change of less than 10 kt in either direction represents no net change. If a TC had made landfall prior to the time point, it was removed from the intensity change calculation and added to the landfall category (bottom row), which is calculated out of 41 cases for the Atlantic and 17 cases for the eastern North Pacific (though no TCs made landfall within 36 h there).

For the Atlantic cases, the Strengthening category contained the fewest events except at t+36 when it equaled the No Change category. Strengthening cases only accounted for 20-26% of over-water cases during the study period. The Weakening category was by far the dominant category at all times, indicating that reductions in intensity are most common in the 36 h

Table 1. Intensity changes following concentric eyewall formation for Atlantic cases. TCs that made landfall prior to the time were removed from the intensity change calculations and placed in the landfall category.

Intensity Change Relative to t+0	***t+12***	***t+24***	***t+36***
Strengthen (≥ 10 kt)	20%	21%	26%
No Change (0-5 kt)	37%	23%	26%
Weaken (≤ -10 kt)	43%	56%	48%
Landfall (/41 cases)	2%	17%	24%

Table 2. Intensity changes following concentric eyewall formation for eastern North Pacific cases. TCs that made landfall prior to the time were removed from the intensity change calculations and placed in the landfall category.

Intensity Change Relative to t+0	***t+12***	***t+24***	***t+36***
Strengthen (≥ 10 kt)	23.5%	23.5%	24%
No Change (0-5 kt)	53%	11.5%	0%
Weaken (≤ -10 kt)	23.5%	65%	76%
Landfall (/41 cases)	0%	0%	0%

following concentric eyewall formation. About 25% of Atlantic cases occurred within 36 h of landfall (as indicated in HURDAT2). In terms of the number of TCs, ten of the 25 Atlantic TCs in the study (40%) made landfall within 36 h of concentric eyewall formation. For six of the ten TCs, the final concentric eyewall was the last one in a series.

The distribution of eastern North Pacific cases among the categories differed substantially from the Atlantic cases. The No Change category was dominant at t+12 with 53% of cases, but decreased to only 11.5% at t+24 and to 0% at t+36. Therefore substantial intensity

changes can be anticipated within 36 h of concentric eyewall formation in the eastern North Pacific. The 24% proportion of Strengthening cases was similar to the Atlantic set. Weakening dominated the distribution at t+24 (65%) and t+36 (76%). One possible cause for the larger proportion of Weakening cases is the rapid cooling of sea surface temperature toward the north and west of the concentric eyewall formation region. Warm ocean water is a key source of energy for TC intensification (Emanuel 1986, Rotunno and Emanuel 1987), so reducing the available energy may induce weakening.

5. Conclusions and Future Work

Two sets of concentric eyewall events have been presented in this paper. The Atlantic set consisted of 41 events from 25 TCs, and the eastern North Pacific set consisted of 17 events from 14 TCs. The formation of sequential concentric eyewalls is far more common over the Atlantic Ocean; 64% of Atlantic TCs developed concentric eyewalls more than once during their lifetimes compared to 21% of eastern North Pacific TCs. All 39 TCs attained major hurricanes status (100 kt) at some point during their lifetimes. Concentric eyewall events are more frequently observed over the Atlantic Ocean, since there are comparable numbers of TCs and of major hurricanes in each region. Concentric eyewall formation tends to occur over the western Atlantic Ocean (including the Caribbean Sea and Gulf of Mexico), and over the eastern half of the eastern North Pacific Ocean near the western coast of Mexico. Events are most frequent in late summer and early autumn, with a peak in late August through late September. Strengthening is not frequently observed after concentric eyewall formation. In both regions, only 20-25% of cases had strengthened at t+12, t+24, and t+36. Weakening was most common at t+24 and t+36 in both regions.

The next step in this research project is to investigate why the intensity changes are occurring. Environmental conditions in the 36 h after concentric eyewall formation will be analyzed to see whether the conditions contribute to the intensity change. Data on environmental conditions is available in real-time to forecasters at the National Hurricane Center, so any relationships from this analysis may be useful operationally. Peripheral to this question is why the eastern North Pacific is apparently less conducive to concentric eyewall formation; one possible reason is the small region of favorable conditions for maintenance of major hurricane intensity.

No studies have directly investigated serial concentric eyewall formation, such as those observed in 2004 with Hurricanes Frances (three events), Ivan (five events), and Karl (three events). When multiple instances of concentric eyewalls occur, the period of lower confidence in forecasts is extended. A related question is why some TCs are at major hurricane intensity for several days, but do not develop concentric eyewalls during these periods. Two examples are Isabel (2003; Lawrence et al. 2005) and Flossie (2007; Avila and Rhome 2009).

Another important point from the analysis presented in this paper is the frequency of landfall after concentric eyewall formation. Ten of the 25 Atlantic TCs made landfall within the 36 h study period. Since hurricane warnings for coastal areas are now issued at 36 h prior to landfall, accurate intensity forecasts are especially critical during this period. Concentric eyewall events near the time of landfall have not been studied well, so these cases will be evaluated more in future work.

6. Acknowledgments

This paper is a summary of research presented at the 2014 Edward F. Hayes Graduate Research Forum in the Mathematical and Physical Sciences Oral Division. It represents preliminary work on the author's dissertation for the doctoral degree through the Atmospheric Sciences Program. The author was supported by a Distinguished University Fellowship from the Graduate School of The Ohio State University during much of the time this work was completed. The National Hurricane Center (www.nhc.noaa.gov) and the Naval Research Labs TC archive (http://www.nrlmry.navy.mil/TC.html) grant public access to their vast quantities of data, making this project feasible. The author would like to thank Dr. Jay Hobgood (adviser) for comments and guidance on the research, and the Council of Graduate Students for staging the Hayes Forum.

7. References

Avila, L. A., and J. Rhome, 2009: Eastern North Pacific Hurricane Season of 2007. *Mon. Wea. Rev.*, **137**, 2436–2447.

Avila, L. A., and J. Cangialosi, 2011: Hurricane Irene Tropical Cyclone Report. National Hurricane Center, 45 pp.

Blake, E. S., and E. J. Gibney, 2011: The deadliest, costliest, and most intense United States tropical cyclones from 1851 to 2010 (and other frequently requested hurricane facts). NOAA Tech. Memo. NWS NHC 6. 49 pp.

Dvorak, V. F., 1975: Tropical cyclone intensity analysis and forecasting from satellite imagery. *Mon. Wea. Rev.*, **103,** 420–430.

Dvorak, V. F., 1984: Tropical cyclone intensity analysis using satellite data. NOAA Tech. Rep. 11, 45 pp.

Emanuel, Kerry A., 1986: An Air-Sea Interaction Theory for Tropical Cyclones. Part I: Steady-State Maintenance. *J. Atmos. Sci.*, **43**, 585–605.

Franklin, J. L., R. J. Pasch, L. A. Avila, J. L. Beven II, M. B. Lawrence, S. R. Stewart, and E. S. Blake, 2006: Atlantic hurricane season of 2004. *Mon. Wea. Rev.*, **134**, 981–1025.

Hawkins, J. D., and M. Helveston, 2004: Tropical cyclone multiple eyewall characteristics. *Extended Abstracts, 26th Conf. on Hurricanes and Tropical Meteorology*, Miami, FL, Amer. Meteor. Soc., P1.7.

Hawkins, J. D., T. F. Lee, J. Turk, C. Sampson, J. Kent, and K. Richardson, 2001: Real–Time Internet Distribution of Satellite Products for Tropical Cyclone Reconnaissance. *Bull. Amer. Meteor. Soc.*, **82**, 567–578.

Hawkins, J. D., M. Helveston, T. F. Lee, F. J. Turk, K. Richardson, C. Sampson, J. Kent, and R. Wade, 2006: Tropical cyclone multiple eyewall configurations. Preprints, *27th Conf. on Hurricanes and Tropical Meteorology*, Monterey, CA, Amer. Meteor. Soc., 6B.1.

Hence, D. A., and R. A. Houze Jr., 2012: Vertical structure of tropical cyclones with concentric eyewalls as seen by the TRMM Precipitation Radar. *J. Atmos. Sci.*, **69**, 1021–1036.

Jarvinen, B. R., C. J. Neumann, and M. A. S. Davis, 1984: A tropical cyclone data tape for the North Atlantic basin, 1886–1983: Contents, limitations, and uses. NOAA Tech. Memo. NWS NHC 22, 21 pp.

Jordan, C. L. and F. J. Schatzle. 1961. The "double eye" of Hurricane Donna. Mon. Wea. Rev. 89:354–356.

Kossin, J. P., and M. Sitkowski, 2009: An Objective Model for Identifying Secondary Eyewall Formation in Hurricanes. *Mon. Wea. Rev.*, **137**, 876–892.

Kuo, H.-C., C.-P. Chang, Y.-T. Yang, and H.-J. Jiang, 2009: Western North Pacific Typhoons with Concentric Eyewalls. *Mon. Wea. Rev.*, **137**, 3758–3770.

Landsea, C. W., and J. L. Franklin, 2013: Atlantic Hurricane Database Uncertainty and Presentation of a New Database Format. *Mon. Wea. Rev.*, **141**, 3576–3592.

Landsea, C. W., and Coauthors, 2004: A Reanalysis of Hurricane Andrew's Intensity. *Bull. Amer. Meteor. Soc.*, **85**, 1699–1712.

Lawrence, M. B., L. A. Avila, J. L. Beven, J. L. Franklin, R. J. Pasch, and S. R. Stewart, 2005: Atlantic Hurricane Season of 2003. *Mon. Wea. Rev.*, **133**, 1744–1773.

Lee, T. F., F. J. Turk, J. Hawkins, and K. Richardson, 2002: Interpretation of TRMM TMI Images of Tropical Cyclones. *Earth Interact.*, **6**, 1–17.

Negri, A. J., R. F. Adler, and C. D. Kummerow, 1989: False-Color Display of Special Sensor Microwave/Imager (SSM/I) Data. *Bull. Amer. Meteor. Soc.*, **70**, 146–151.

Rappaport, E. N., and Coauthors, 2009: Advances and Challenges at the National Hurricane Center. *Wea. Forecasting*, **24**, 395–419.

Rotunno, Richard, Kerry A. Emanuel, 1987: An Air–Sea Interaction Theory for Tropical Cyclones. Part II: Evolutionary Study Using a Nonhydrostatic Axisymmetric Numerical Model. *J. Atmos. Sci.*, **44**, 542–561.

Schneider, C.A., W. S. Rasband, and K. W. Eliceiri, 2012: "NIH Image to ImageJ: 25 years of image analysis". *Nature Methods*, **9**, 671-675.

Sitkowski, M., J. P. Kossin, and C. M. Rozoff, 2011: Intensity and Structure Changes during Hurricane Eyewall Replacement Cycles. *Mon. Wea. Rev.*, **139**, 3829–3847.

Velden, C., and Coauthors, 2006: The Dvorak tropical cyclone intensity estimation technique: A satellite-based method that has endured for over 30 years. *Bull. Amer. Meteor. Soc.*, **87**, 1195–1209.

Willoughby, H. E., and P. G. Black, 1996: Hurricane Andrew in Florida: Dynamics of a Disaster. *Bull. Amer. Meteor. Soc.*, **77**, 543–549.

Willoughby, H., J. Clos, and M. Shoreibah, 1982: Concentric eye walls, secondary wind maxima, and the evolution of the hurricane vortex. *J. Atmos. Sci.*, **39**, 242–264.

Yang, Y.-T., H.-C. Kuo, E. A. Hendricks, and M. S. Peng, 2013: Structural and Intensity Changes of Concentric Eyewall Typhoons in the Western North Pacific Basin. *Mon. Wea. Rev.*, **141**, 2632–2648.